

## Two New Dinuclear Sterically Crowded Cu<sup>II</sup> Complexes as Catalyst Precursors for the Oxidative Coupling of 2,6-Dimethylphenol

Guillem Aromí,<sup>[a]</sup> Patrick Gamez,<sup>[a]</sup> Huub Kooijman,<sup>[b]</sup> Anthony L. Spek,<sup>[b]</sup>  
Willem L. Driessen,<sup>[a]</sup> and Jan Reedijk\*<sup>[a]</sup>

**Keywords:** Copper / N ligands / Homogeneous catalysis / Oxidations

The molecular structure and spectroscopic properties of the first two bis( $\mu$ - $\eta^1$ -nitrate)-bridged, dinuclear Cu complexes containing 4,4'-biimidazole ligands are presented. <sup>1</sup>H NMR, EPR, and UV/Vis spectroscopy indicate that their solid-state structure is not retained in solution. Dioxygen uptake measurements show that the presence of a methyl group at the 2-position of the imidazole rings leads to a dramatic increase of the rate of the catalytic polymerization of 2,6-dimethyl-

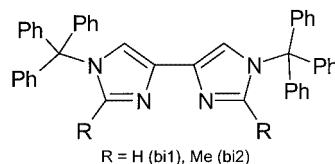
phenol. Detailed examination of the molecular structures of both catalyst precursors in the crystalline state suggests that this may either be caused by the difference in basicity of the biimidazole ligands or by a small but important steric effect of the 2-Me groups affecting the coplanarity of equatorial Cu<sup>II</sup> ligands and the orientation of the axial nitrate ligands. (© Wiley-VCH Verlag GmbH & Co. KGaA, 69451 Weinheim, Germany, 2003)

### Introduction

Our longstanding interest in the preparation and spectroscopic study of copper coordination compounds with azole-based ligands<sup>[1–6]</sup> originates from two main driving forces. First, it is well established that many important enzymes hold a copper-active site mainly by means of the imidazole moieties from protein histidine amino acids.<sup>[7]</sup> Second, the unique characteristics of the Cu<sup>II</sup>/Cu<sup>I</sup> redox couple render many of their complexes especially suited for the catalysis of organic oxidation reactions, in some cases with industrial relevance.<sup>[8]</sup>

Since its discovery in 1959,<sup>[9]</sup> the oxidative polymerization of 2,6-dimethylphenol (DMP) catalyzed by Cu complexes of N-based ligands has been used on an industrial scale. The product, poly(1,4-phenylene ether) (PPE), is a valuable thermoplastic with vast worldwide applications thanks to its excellent mechanical properties and chemical resistance.<sup>[10,11]</sup> An unwanted side product of this reaction is diphenoquinone (DPQ), which results from the C–C coupling and subsequent oxidation of two DMP units. Considerable research effort has been dedicated to improve the performance and selectivity of the reaction and to elucidate its mechanism. For example, we have recently found conditions that have led to a dramatic increase of the reac-

tion rates compared with those still encountered in large-scale production.<sup>[12]</sup> Although the exact mechanism of the reaction remains a matter of discussion, several hypotheses have been put forward. Early proposals favored a pathway involving phenoxy radicals as key intermediates.<sup>[13,14]</sup> More recently, the presence of a dinuclear phenolate-bridged Cu<sup>II</sup> complex has been suggested.<sup>[15–17]</sup> Quite diverse approaches have been adopted to obtain mechanistic details of the reaction. These include kinetic studies using various kinds of ligands,<sup>[18–24]</sup> the use of different substrates such as oligomers,<sup>[16]</sup> ab initio calculations,<sup>[25]</sup> or changing the proportions between the various components (Cu, ligand, base, water, substrate) and studying the influence on the catalytic activity.<sup>[12,19,26]</sup> Another strategy has been to examine the molecular structure of various catalyst precursors or potential reaction intermediates to establish possible correlations between geometric parameters and activity. In this context, we decided to explore the coordination properties of the two chelating 4,4'-biimidazole (bi) ligands shown in Scheme 1.<sup>[27]</sup>



Scheme 1

In sharp contrast to their isomeric 2,2'-analogues, 4,4'-biimidazole chelates have not been found as part of any structurally characterized coordination compound, most likely owing to the difficulty in preparing these ligands. In

<sup>[a]</sup> Leiden Institute of Chemistry, Gorlaeus Laboratories, Leiden University, P. O. Box 9502, 2300 RA Leiden, The Netherlands  
Fax: (internat.) + 31-71/527-4671  
E-mail: reedijk@chem.leidenuniv.nl

<sup>[b]</sup> Bijvoet Center for Biomolecular Research, Crystal and Structural Chemistry, Utrecht University, Padualaan 8, 3584 CH, Utrecht, The Netherlands

this paper we report synthetic procedures to prepare the complexes  $[\text{Cu}(\mu\text{-}\eta^1\text{-NO}_3)(\text{NO}_3)(\text{bi})_2]$  [ $\text{bi} = \text{bi1}$  (**1**),  $\text{bi2}$  (**2**)], the first examples containing 4,4'-biimidazole ligands. Their catalytic activity during the oxidation of DMP into PPE is examined and discussed in the light of their single-crystal X-ray structure and their solution properties.

## Results and Discussion

Complexes **1** and **2** both crystallize from acetonitrile directly from reaction mixtures containing the stoichiometric amount of the appropriate components. In both cases, well-formed crystals collapse immediately upon exposure to air, probably reflecting loss of lattice solvent, which is detected crystallographically, but not from microanalysis (see below). The fact that the complexes are hygroscopic is reflected in repeated experiments of elemental analysis.

### Description of the Structures

Crystallographic data for  $[\text{Cu}(\mu\text{-}\eta^1\text{-NO}_3)(\text{NO}_3)(\text{bi1})_2]$  (**1**) and  $[\text{Cu}(\mu\text{-}\eta^1\text{-NO}_3)(\text{NO}_3)(\text{bi2})_2]$  (**2**) are collected in Table 4. Selected interatomic distances and angles for complexes **1** and **2** are listed in Table 1 and the respective molecular structures are represented in Figures 1 and 2.

Table 1. Selected interatomic distances [Å] and angles [°] for  $[\text{Cu}(\mu\text{-}\eta^1\text{-NO}_3)(\text{NO}_3)(\text{bi1})_2]$  (**1**) and  $[\text{Cu}(\mu\text{-}\eta^1\text{-NO}_3)(\text{NO}_3)(\text{bi2})_2]$  (**2**)

<b>1</b>		<b>2</b>	
Cu(1)–O(91)	2.403(3)	Cu(1)–O(91)	1.9754(15)
Cu(1)–N(21)	2.002(3)	Cu(1)–N(21)	1.9781(19)
Cu(1)–O(96)	1.970(3)	Cu(1)–O(96)	1.9626(17)
Cu(1)–O(91)a	1.996(3)	Cu(1)–O(91)a	2.3598(17)
Cu(1)–O(97)	2.643(5)	Cu(1)–O(97)	2.6972(23)
Cu(1)–N(11)	1.996(3)	Cu(1)–N(11)	1.9728(17)
Cu(1)⋯Cu(1)a	3.4106(8)	Cu(1)⋯Cu(1)a	3.530(1)
O(91)–Cu(1)–O(96)	93.37(7)	O(91)–Cu(1)–O(96)	94.43(12)
O(91)–Cu(1)–N(21)	91.54(7)	O(91)–Cu(1)–N(21)	97.76(12)
O(96)–Cu(1)–N(11)	93.66(7)	O(96)–Cu(1)–N(11)	96.06(12)
N(11)–Cu(1)–N(21)	81.60(8)	N(11)–Cu(1)–N(21)	83.24(12)
O(91)–Cu(1)–O(91)a	76.60(6)	O(91)–Cu(1)–O(91)a	73.64(10)
O(96)–Cu(1)–N(21)	174.29(7)	O(96)–Cu(1)–N(21)	167.80(15)
N(11)–Cu(1)–O(91)a	100.22(7)	N(11)–Cu(1)–O(91)a	169.28(13)
O(91)–Cu(1)–N(11)	172.34(8)	O(91)–Cu(1)–N(11)	95.95(12)
O(96)–Cu(1)–O(91)a	91.17(6)	O(96)–Cu(1)–O(91)a	87.46(11)
N(21)–Cu(1)–O(91)a	92.80(7)	N(21)–Cu(1)–O(91)a	95.44(11)
Cu(1)–O(91)–Cu(1)a	103.40(6)	Cu(1)–O(91)–Cu(1)a	106.36(11)

### $[\text{Cu}(\mu\text{-}\eta^1\text{-NO}_3)(\text{NO}_3)(\text{bi1})_2]$ (**1**)

The structure of **1** shows a dinuclear centrosymmetric complex consisting of two Cu<sup>II</sup> ions bridged by two monodentate  $\mu\text{-}\eta^1\text{-NO}_3^-$  ligands. This bridging mode is relatively uncommon for nitrate,<sup>[28]</sup> which usually bridges Cu ions in a didentate fashion. The bridging nitrate ligand is bound to the Cu centers through a short [1.975(2) Å] and a long bond [2.360(2) Å], which occupy an equatorial and an axial posi-

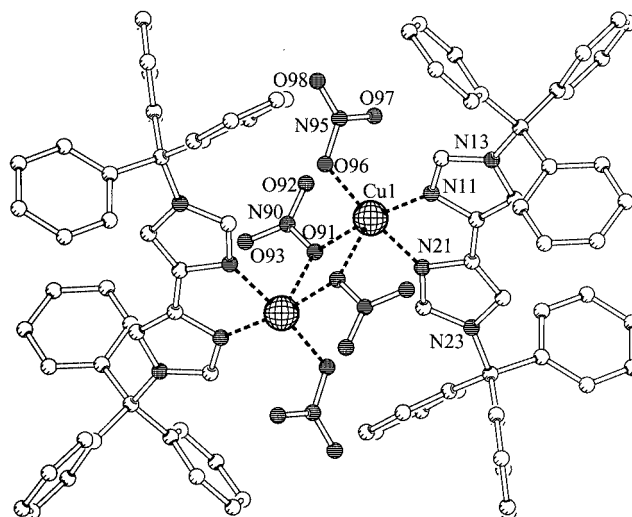


Figure 1. PLATON<sup>[38]</sup> representation of  $[\text{Cu}(\mu\text{-}\eta^1\text{-NO}_3)(\text{NO}_3)(\text{bi1})_2]$  (**1**)

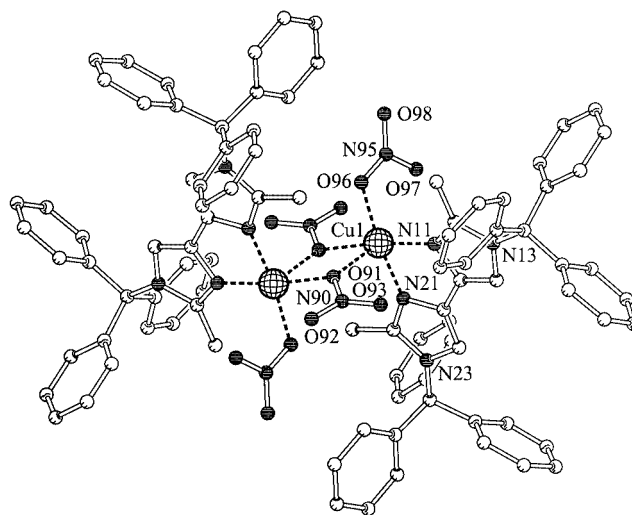


Figure 2. PLATON<sup>[38]</sup> representation of  $[\text{Cu}(\mu\text{-}\eta^1\text{-NO}_3)(\text{NO}_3)(\text{bi2})_2]$  (**2**)

tion, respectively, of the nearly square-pyramidal coordination environment observed around the Cu centers ( $\tau = 0.03$ , where  $\tau$  is 0 and 1 for the perfect square-pyramidal and trigonal-bipyramidal geometries, respectively).<sup>[29]</sup> The remaining equatorial positions of each metal ion are completed by the N donors of one chelating bi1 ligand [at distances of 1.973(2) and 1.978(2) Å, respectively] and by one O atom of a terminal  $\text{NO}_3^-$  ligand [1.963(2) Å]. A second O atom of the latter lays 2.697(2) Å apart from the Cu<sup>II</sup> ion. The intermetallic Cu⋯Cu distance is 3.4106(8) Å. The crystal packing shows no unusual features. Complexes **1** and **2** (vide infra) are the first crystallographically characterized complexes of a 4,4'-biimidazole ligand.

### $[\text{Cu}(\mu\text{-}\eta^1\text{-NO}_3)(\text{NO}_3)(\text{bi2})_2]$ (**2**)

Complex **2** is isostructural with complex **1**. The presence of a methyl substituent at the 2- and 2'-positions of the imidazole rings does not appear to affect significantly the

overall structure of the complex. The metal centers maintain the square-pyramidal coordination geometry (with  $\tau = 0.02$ ), and are slightly more separated [ $\text{Cu}\cdots\text{Cu} = 3.530(1)$  Å] than in **1**. The bridging nitrate ligand is bound to the Cu centres at 1.996(3) and 2.403(3) Å, and the oxygen donor of the terminal nitrate group is separated from the metal ion by 1.970(3) Å. The long  $\text{O}\cdots\text{Cu}$  contact featured by this ligand is 2.643(5) Å. The orientations of the nonbridging nitrate groups do differ from complex **1**, which is ascribed to the steric effect of the 2-Me group. The chelating ligands display Cu–N distances of 1.996(3) and 2.002(3) Å.<sup>[30,31]</sup> The packing in this structure is also uneventful and involves mainly van der Waals forces.

### Spectroscopic Studies

The infrared (IR) spectra of complexes **1** and **2** were measured in the solid state. Both compounds exhibit a strong absorption (1279 and 1282  $\text{cm}^{-1}$ , respectively) in the region characteristic for  $\nu(\text{NO})$  of monodentate-coordinated nitrates.<sup>[32]</sup>

The electronic spectra of **1** and **2** were collected from polycrystalline samples, using the diffuse reflectance technique. Both spectra have the same qualitative appearance, with the bands of complex **1** being slightly red-shifted with respect to those of **2**. One broad absorption band is observed (Table 2) in the 712–770-nm range (14000–12900  $\text{cm}^{-1}$ ) that can be assigned to d–d transitions involving the  $\text{Cu}^{\text{II}}$  ion in a square-pyramidal environment.<sup>[33,34]</sup> Near-ultraviolet absorption bands at ca. 400 nm (25000  $\text{cm}^{-1}$ , shoulder; **1**) and 452 nm (22000  $\text{cm}^{-1}$ ; **2**) were also detected, and are assigned as charge-transfer transitions from a nitrate nonbonding orbital to the copper ion. In addition, both spectra display LMCT transitions from the chelating

ligands at ca. 320 and 261 nm (31100 and 38100  $\text{cm}^{-1}$ ; **1**) and at ca. 320 and 274 nm (31100 and 36300  $\text{cm}^{-1}$ ; **2**). The electronic spectra of both compounds were also measured in  $\text{CH}_2\text{Cl}_2$  solution. The above-mentioned various bands were found at very similar positions, but a dramatic decrease of intensity of the visible absorptions with respect to the ultraviolet bands was evident. This could be due to a change of the dipolar integral for some transitions, caused by an alteration of the symmetry within the complex upon dissolution or by dissociation. Furthermore, a new band could be seen at very high energy (227 nm, i.e. 43800  $\text{cm}^{-1}$  for both complexes), most probably corresponding to an intra-ligand transition.

Complexes **1** and **2** were studied by paramagnetic  $^1\text{H}$  NMR in  $\text{CDCl}_3$  solution (Figure 3). A list of the chemical shifts of the different observed resonances is included in Table 2. Both complexes show a unique set of three paramagnetically broadened signals in the range  $\delta = 6\text{--}8$  ppm, corresponding to the phenyl rings of the biimidazole ligands. Complex **2** also displays a very broadened and shifted resonance at  $\delta \approx -9$  ppm attributed to the methyl substituents on the imidazole rings of the ligand bi2. The signals corresponding to the protons directly on the imidazole rings were broadened beyond detection. Thus, the spectra of **1** and **2** show that both complexes exhibit higher symmetry in solution than in the solid state. This could be due to a rapid fluxional process rendering both halves of the ligand equivalent, or to the dissociation of the dimers in solution, leading to more symmetric mononuclear species. The second hypothesis was supported by a variable temperature  $^1\text{H}$  NMR study, conducted down to ca. 110 K, in which no sign of any de-coalescence process could be observed (data not shown).

The solid-state and solution X-band EPR spectra of **1** and **2**, respectively, were compared at room temperature and ca. 77 K. The solution ( $\text{CH}_2\text{Cl}_2/\text{toluene}$ , 2:1) spectrum

Table 2. Spectroscopic data for complexes **1** and **2**

	Complex 1	Complex 2
Ligand field (solid) <sup>[a]</sup>	38100, 31100, ca. 25500, 13900	36300, ca. 31100, 22000, 13300
Ligand field (solution) <sup>[b]</sup>	43800, 39300, 25500, 14000	43800, 38100, 22000, 12900
EPR (solution) <sup>[c]</sup>	$g_{\text{iso}} = 2.15$	$g_{\text{iso}} = 2.16$
EPR (frozen solution) <sup>[d]</sup>	$g_{\parallel} = 2.30$ ( $A_{\parallel} = 166$ G), $g_{\perp} = 2.07$	$g_{\parallel} = 2.31$ ( $A_{\parallel} = 150$ G), $g_{\perp} = 2.07$
EPR (solid) <sup>[e]</sup>	$g = 2.05$	$g = 2.11$
300 MHz $^1\text{H}$ NMR <sup>[f]</sup>	7.41 ( <i>m</i> -Ph), 7.05 ( <i>p</i> -Ph), 6.44 ( <i>m</i> -Ph)	7.47 ( <i>m</i> -Ph), 7.04 ( <i>p</i> -Ph), 6.51 ( <i>m</i> -Ph), ca. -9 ( $\text{CH}_3$ )

<sup>[a]</sup> In  $\text{cm}^{-1}$ , registered in solid state at 298 K, diffuse reflectance. <sup>[b]</sup> In  $\text{cm}^{-1}$ , registered in  $\text{CH}_2\text{Cl}_2$  solutions at 298 K. <sup>[c]</sup> At 77 K, frozen solution in  $\text{CH}_2\text{Cl}_2/\text{toluene}$  (2:1). At 298 K, solution in  $\text{CH}_2\text{Cl}_2/\text{toluene}$  (2:1). <sup>[d]</sup> At 77 K, frozen solution in  $\text{CH}_2\text{Cl}_2/\text{toluene}$  (2:1). <sup>[e]</sup> At 77 K, polycrystalline sample. <sup>[f]</sup> In ppm, in  $\text{CDCl}_3$ .

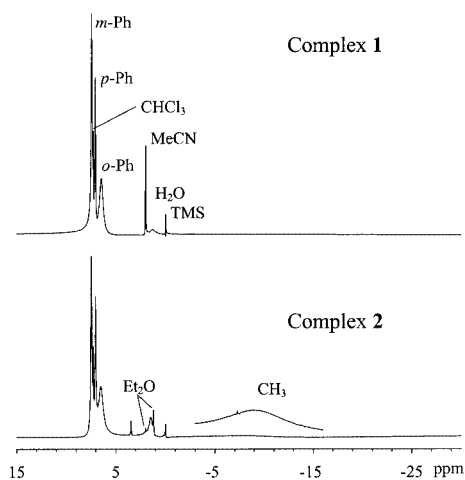


Figure 3. 300 MHz  $^1\text{H}$  NMR spectra of complexes **1** and **2** in  $\text{CDCl}_3$ ; the labels used for the top spectrum apply also to the bottom spectrum

at room temperature (not shown) displays for both species a band typical for mononuclear Cu<sup>II</sup>, with  $g_{\text{iso}} = 2.15/2.16$  (1/2). Both bands are split into four signals ( $A_{\text{iso}} = 68/62$  G) due to hyperfine coupling of the spin with the Cu nuclei ( $I = 3/2$ ). In frozen solution, both compounds feature typical axial spectra (Figure 4) where  $g_{\parallel} = 2.30/2.31$  and  $g_{\perp} = 2.07/2.07$ . From these values, the isotropic  $g$  constants reported above can be calculated from  $g_{\text{iso}} = 1/3(2 \times g_{\perp} + g_{\parallel})$ . The parallel resonance in both compounds display hyperfine splitting due to the coupling with Cu ( $A_{\parallel} = 166/150$  G). Also, both spectra show superhyperfine splitting of the perpendicular signal due to interaction with the <sup>14</sup>N nuclei of the biimidazole ligands. These spectra are consistent with the presence of mononuclear species in solution. A possible distribution of species could be tetragonally elongated [Cu(NO<sub>3</sub>)<sub>2</sub>(bi)<sub>2</sub>] along with solvated Cu(NO<sub>3</sub>)<sub>2</sub>. Because  $A_{\parallel}$  in **1** is slightly higher than in **2** the first type of species may well be EPR-active in both systems, the complex of **2** experiencing a larger distortion from planarity at the equatorial plane caused by the methyl substituents of bi2. A much broader signal underlying the spectra (especially visible in the frozen solution spectrum of **2**) could be attributed to the second type of species. The solid-state EPR spectra of **1** and **2** are also very similar to each other and distinct from the corresponding solution spectra. In both cases, a broad, isotropic signal is observed at  $g = 2.05/2.11$ . These bands could be ascribed to a triplet state, and the dramatic difference with the frozen solution spectra clearly indicates that the dinuclear structure of **1** and **2** observed in the solid state is not maintained in solution. No attempts were made to analyze the triplet signals in detail.

### Catalytic Properties

[Cu( $\mu$ - $\eta^1$ -NO<sub>3</sub>)(NO<sub>3</sub>)(bi1)<sub>2</sub>] (**1**) and [Cu( $\mu$ - $\eta^1$ -NO<sub>3</sub>)(NO<sub>3</sub>)(bi2)<sub>2</sub>] (**2**) were tested as catalysts for the polymerization of 2,6-dimethylphenol (DMP) to ascertain the influence of the ligand derivatives on the catalytic activity of these precursors, in relation to their structural properties. Interestingly, the catalytic activity of complex **2** (which contains the 2,2'-dimethylbiimidazole ligand) is more than ten times faster than that of **1** (Table 3). This confirms the results achieved with ligands Meim and Dmeim (1-methylimidazole and 1,2-dimethylimidazole, respectively), where a methyl group on the 2-position of the imidazole ring led to a dramatic enhancement of activity<sup>[18]</sup> (see Table 3). The crystal structures of complexes **1** and **2** (see above) have

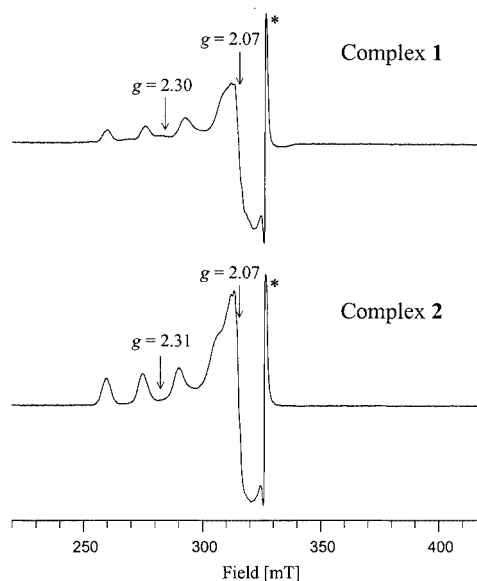


Figure 4. X-band EPR spectra of complexes **1** and **2** at 77 K in CH<sub>2</sub>Cl<sub>2</sub>/toluene (2:1) frozen solution; the signal labeled “\*” corresponds to the reference radical used for calibration (see Exp. Sect.)

revealed that the presence of methyl groups at the 2,2'-positions of the imidazole rings has almost no influence on the metric parameters of the rest of the complex. This suggests that the main reason for the difference in activity is the differential basicity of the ligands. It has been proposed that the N-based ligands of the catalyst might act as a Brønsted base during the catalytic cycle. In such a case the  $pK_b$  of the ligand could affect the rate of conversion. In this particular system the structural factors influencing the catalytic activity might be dominated by the much larger triphenylmethyl substituents common to both compounds. It would be interesting to expand the present study using the corresponding ligands 4,4'-biimidazole and 2,2'-dimethyl-4,4'-biimidazole. Here, however, an influence of the steric properties on the catalytic activity cannot be completely excluded, since no structural details of intermediates containing the reaction substrate, DMP, are known.

### Conclusion

Single-crystal X-ray diffraction has revealed the solid-state molecular structure of the two copper dimeric com-

Table 3. Catalytic activity of Cu<sup>II</sup> with didentate ligands bi1 and bi2 during the polymerization of DMP in acetonitrile, compared with that with Meim and Dmeim<sup>[18]</sup>

Ligand L	L/Cu	Conversion [%]	Reaction time [h]	$R_0$ [ $10^{-5}$ molL <sup>-1</sup> s <sup>-1</sup> ]	PPE [%]
bi1	1	68	1.50	3	95.1
bi2	1	43	0.30	31	95.0
Meim <sup>[a]</sup>	4	68	0.08	142	> 95
Dmeim <sup>[b]</sup>	4	76	0.08	200	> 95

<sup>[a]</sup> Meim = 1-methylimidazole. <sup>[b]</sup> Dmeim = 1,2-dimethylimidazole.

plexes  $[\text{Cu}(\mu\text{-}\eta^1\text{-NO}_3)(\text{NO}_3)(\text{bi1})_2]$  (**1**) and  $[\text{Cu}(\mu\text{-}\eta^1\text{-NO}_3)(\text{NO}_3)(\text{bi2})_2]$  (**2**) are similar, despite the fact that the 2-Me group of the latter is close to the coordination sphere of  $\text{Cu}^{\text{II}}$ . These are the first crystallographically characterized coordination compounds featuring 4,4'-biimidazole ligands. Spectroscopic studies indicate that the solid-state structure of compounds **1** and **2** is not preserved in solution. The various data suggest that dissociation into mononuclear species takes place. Complexes **1** and **2** have been used as catalyst precursors for the oxidative coupling of DMP into PPE. In view of the solid-state molecular structure of both precursors, their dramatic difference in activity is interpreted in terms of the difference in ligand basicity. The EPR solution spectra, however, indicate that the presence of an Me group might distort the mononuclear complexes present in solution, thereby affecting their catalytic activity. The preparation and crystallographic characterization of additional catalyst precursors for this reaction will establish any correlations between structural parameters and the catalytic activity of these species.

## Experimental Section

**General Remarks:** The biimidazole ligands 1,1'-bis(triphenylmethyl)-4,4'-biimidazole (bi1) and 2,2'-dimethyl-1,1'-bis(triphenylmethyl)-4,4'-biimidazole (bi2) were prepared according to the method reported by Pyne et al.<sup>[27]</sup> Solvents and chemicals were commercially available and were used as received unless otherwise indicated. The syntheses of all organic compounds were performed under argon and their purification was commonly performed in air. Infrared spectra were collected with a Perkin–Elmer Paragon 1000 spectrophotometer equipped with a Golden Gate Diamond ATR as a sample support.  $^1\text{H}$  NMR spectra were recorded with a 200 MHz Jeol JNM FX-200 instrument and a 300 MHz Bruker DPX 300 spectrometer. Vis/NIR spectra were measured with a Perkin–Elmer Lambda 900 spectrophotometer in  $\text{CH}_2\text{Cl}_2$  solution or using the diffuse reflectance technique, with  $\text{MgO}$  as a reference. X-band EPR spectra were recorded with a JEOL ESR spectrometer equipped with an Esprit 330 data system at room temperature and at 77 K, with dpph as an internal reference ( $g = 2.0036$ ). Elemental analyses were performed at the Microanalytical Laboratory of the University College, Dublin, Ireland or at the Mikroanalytisches Labor Pascher, Remagen-Bandorf, Germany.

**Dioxygen Uptake Measurements:** In a typical quantitative, time-resolved dioxygen-uptake experiment, one compartment of a special in-house made two-compartment reaction vessel was filled with 5 mL of a 0.01 M  $\text{Cu}^{\text{II}}$ /ligand solution, and the other with 10 mL of the substrate (3 mmol) solution. Intense shaking in under dioxygen combined these solutions and started the reaction. The resulting reaction mixture was 3.33 mM in Cu and 0.2 M in DMP (**3**). The polymerization reactions were performed at 25 °C under pure dioxygen at atmospheric pressure. In this particular case, a ligand/Cu ratio of 1 and a NaOMe/Cu ratio of 2 were used. The catalytic activity was determined from the initial dioxygen-uptake rate  $R_0$ . A detailed description of the dioxygen-uptake experiments and the processing of the experimental data have been previously published.<sup>[35]</sup>

**$[\text{Cu}(\mu\text{-}\eta^1\text{-NO}_3)(\text{NO}_3)(\text{bi1})_2]$  (**1**):** A slurry of bi1 (62 mg, 0.1 mmol) in MeCN (5 mL) was added to a stirred blue solution of  $\text{Cu}(\text{NO}_3)_2 \cdot 3\text{H}_2\text{O}$  (26 mg, 0.1 mmol) in MeCN (5 mL). The ligand dissolved completely upon reaction. After a few minutes, the blue solution was left unperturbed and the solvent was allowed to slowly evaporate for a few days. After this time, blue block-shaped crystals suitable for X-ray crystallography had deposited. The crystals were collected by filtration and dried in vacuo. The yield was 44%. IR (neat):  $\tilde{\nu}$  [ $\text{cm}^{-1}$ ] = 1511.8 m, 1490.0 m, 1471.6 s, 1445.7 m, 1278.9 vs, 1214.0 m, 1085.8 m, 1002.1 m, 947.3 w, 845.8 w, 744.6 vs, 697.7 vs, 659.4 vs, 638.8 m, 374.0 w, 345.3 m, 316.6 w.  $\text{C}_{88}\text{H}_{68}\text{Cu}_2\text{N}_{12}\text{O}_{12}(\text{H}_2\text{O})_2$  (1648.72): calcd. C 64.11, H 4.40, N 10.19; found C 63.86, H 4.12, N 9.96.

**$[\text{Cu}(\mu\text{-}\eta^1\text{-NO}_3)(\text{NO}_3)(\text{bi2})_2]$  (**2**):** A slurry of bi2 (259 mg, 0.4 mmol) in MeCN (10 mL) was added to a stirred blue solution of  $\text{Cu}(\text{NO}_3)_2 \cdot 3\text{H}_2\text{O}$  (96 mg, 0.4 mmol) in MeCN (20 mL). After a few minutes, the resulting green solution was filtered with paper and the filtrate was left unperturbed for the slow evaporation of the solvent. After a few days, green needles suitable for X-ray crystallography were obtained. The solid was collected by filtration and turned gray upon contact with air. The sample was dried in vacuo (yield 31%). IR (neat):  $\tilde{\nu}$  [ $\text{cm}^{-1}$ ] = 1489.7 s, 1446.0 m, 1394.1 w, 1281.8 vs, 1232.9 m, 1149.5 w, 1010.1 m, 747.9 vs, 700.1 vs, 668.2 m, 655.7 w, 637.9 m, 586.0 w, 499.4 w, 398.2 w, 336.4 w.  $\text{C}_{92}\text{H}_{76}\text{Cu}_2\text{N}_{12}\text{O}_{12}(\text{H}_2\text{O})$  (1686.81): calcd. C 65.51, H 4.66, N 9.96; found C 65.67, H 4.78, N 9.48.

**X-ray Crystallography:** Crystals of complexes **1** and **2** were mounted on Lindemann glass capillaries and transferred into the cold nitrogen stream of a Nonius KappaCCD diffractometer on a rotating anode, (Mo- $K_\alpha$  radiation, graphite monochromator,  $\lambda = 0.71073$  Å,  $T = 150$  K). Pertinent data for the structure determinations are collected in Table 4. Structures were solved with direct methods using SHELXS86.<sup>[36]</sup> Refinement on  $F^2$  was performed with SHELXL-97-2.<sup>[37]</sup> The hydrogen atoms were included in the refinement on calculated positions riding on their carrier atoms. The non-hydrogen atoms were refined with anisotropic thermal parameters. The hydrogen atoms were refined with a fixed isotropic displacement parameter related to the value of the equivalent isotropic displacement parameter of their carrier atoms. The structures of both **1** and **2** contain an area filled with acetonitrile. In **1** the solvent could be described with an ordered model, albeit with relatively high displacement parameters. In **2** the volume of the solvent area was significantly larger, and no satisfactory model could be constructed. Therefore, for this complex, the contribution to the structure factors associated with the solvent was taken into account using the SQUEEZE procedure as incorporated in PLATON.<sup>[38]</sup> A total of 126 electrons were found in a system of channels running parallel to  $a$  and  $c$  of  $600$  Å<sup>3</sup> per unit cell, corresponding to approximately six molecules of acetonitrile. The nitrate ions and one of the phenyl rings of **2** displayed high anisotropy in their displacement factors. Mild rigid bond restraints were applied to ensure realistic values for the displacement parameters. Neutral atom scattering factors and anomalous dispersion corrections were taken from the International Tables for Crystallography.<sup>[39]</sup> Geometrical calculations and illustrations were performed with PLATON.<sup>[38]</sup> CCDC-194207 (**1**) and -194208 (**2**) contain the supplementary crystallographic data for this paper. These data can be obtained free of charge at [www.ccdc.cam.ac.uk/conts/retrieving.html](http://www.ccdc.cam.ac.uk/conts/retrieving.html) [or from the Cambridge Crystallographic Data Centre, 12 Union Road, Cambridge CB2 1EZ, UK; Fax: (internat.) + 44-1223/336-033; E-mail: [deposit@ccdc.cam.ac.uk](mailto:deposit@ccdc.cam.ac.uk)].

Table 4. Crystallographic data for [Cu(μ-η<sup>1</sup>-NO<sub>3</sub>)(NO<sub>3</sub>)(bi1)]<sub>2</sub> (1) and [Cu(μ-η<sup>1</sup>-NO<sub>3</sub>)(NO<sub>3</sub>)(bi2)]<sub>2</sub> (2)

	1	2
Crystal data:		
Empirical formula	C <sub>88</sub> H <sub>68</sub> Cu <sub>2</sub> N <sub>12</sub> O <sub>12</sub> ·4C <sub>2</sub> H <sub>3</sub> N	C <sub>92</sub> H <sub>76</sub> Cu <sub>2</sub> N <sub>12</sub> O <sub>12</sub> ·6C <sub>2</sub> H <sub>3</sub> N <sup>[a]</sup>
Formula mass [g·mol <sup>-1</sup> ]	1776.86	1915.09 <sup>[a]</sup>
Crystal system	triclinic	triclinic
Space group	<i>P</i> $\bar{1}$ (no. 2)	<i>P</i> $\bar{1}$ (no. 2)
<i>a</i> [Å]	13.4436(15)	11.286(2)
<i>b</i> [Å]	13.5376(10)	15.320(2)
<i>c</i> [Å]	13.944(3)	15.520(3)
$\alpha$ [°]	90.437(17)	105.442(12)
$\beta$ [°]	118.674(11)	99.655(10)
$\gamma$ [°]	94.982(10)	106.171(10)
<i>V</i> [Å <sup>3</sup> ]	2214.6(5)	2397.9(7)
$\rho_{\text{calcd.}}$ [g·cm <sup>-3</sup> ]	1.332	1.326 <sup>[a]</sup>
<i>Z</i>	1	1
<i>F</i> (000)	922	998 <sup>[a]</sup>
<i>T</i> [K]	150	150
$\mu$ [mm <sup>-1</sup> ] (Mo- <i>K</i> $\alpha$ )	0.552	0.538 <sup>[a]</sup>
Crystal colour	blue	blue–green
Crystal size [mm]	0.1 × 0.3 × 0.3	0.2 × 0.3 × 0.3
Data collection:		
$\theta_{\text{min}}$ , $\theta_{\text{max}}$ [°]	1.6, 27.46	1.6, 25.25
X-ray exposure [h]	1.8	2.4
Data set	–17:17, –17:17, –18:18	–13:12, –18:17, –18:18
Total data	29969	22466
Total unique data	10077	8443
<i>R</i> <sub>int</sub>	0.0699	0.0529
<i>R</i> <sub>σ</sub>	0.0548	0.0452
Absorption correction range	0.864–0.977 [MULABS] <sup>[38]</sup>	4
Refinement:		
No. of refined parameters	570	534
Final <i>R</i> <sup>[b]</sup>	0.0458 [8188 I > 2σ(I)]	0.0618 [7237 I > 2σ(I)]
Final <i>wR</i> <sup>[c]</sup>	0.1243	0.1622
Goodness of fit	1.030	1.045
<i>w</i> <sup>-1</sup> <sup>[d]</sup>	$\sigma^2(F_{\text{obs}}^2) + (0.0597P)^2 + 1.34P$	$\sigma^2(F_{\text{obs}}^2) + (0.0582P)^2 + 5.48P$
( $\Delta/\sigma$ ) <sub>av</sub> , ( $\Delta/\sigma$ ) <sub>max</sub>	< 0.001, 0.001	< 0.001, 0.001
Min., max. residual density [e·Å <sup>-3</sup> ]	–0.76, 0.63	–0.54, 0.66

<sup>[a]</sup> Including the estimated contribution of the disordered solvent. <sup>[b]</sup>  $R1 = \sum ||F_o| - |F_c|| / \sum |F_o|$ . <sup>[c]</sup>  $wR2 = \{\sum [w(F_o^2 - F_c^2)^2] / \sum [w(F_o^2)^2]\}^{1/2}$ . <sup>[d]</sup>  $P = [\text{Max}(F_o^2, 0) + 2F_c^2] / 3$ .

## Acknowledgments

Financial support by the European Union, under contract HPMF-CT-1999-00113 (Marie Curie Fellowship) to G. A. and COST Action D21/003/2001 (P. G.), the Dutch National Research School Combination Catalysis (HRSMC and NIOK) the WFMO (J. R.) and the CW-NWO (A. L. S.) are thankfully acknowledged.

- <sup>[1]</sup> M. Zoeteman, E. Bouwman, R. A. G. De Graaff, W. L. Driessen, J. Reedijk, P. Zanello, *Inorg. Chem.* **1990**, *29*, 3487.  
<sup>[2]</sup> G. J. A. A. Koolhaas, W. L. Driessen, J. Reedijk, J. L. Van der Plas, R. A. G. De Graaff, D. Gatteschi, H. Kooijman, A. L. Spek, *Inorg. Chem.* **1996**, *35*, 1509.  
<sup>[3]</sup> G. J. A. A. Koolhaas, P. M. Van Berkel, S. C. Van der Slot, G. MendozaDiaz, W. L. Driessen, J. Reedijk, H. Kooijman, N. Veldman, A. L. Spek, *Inorg. Chem.* **1996**, *35*, 3525.  
<sup>[4]</sup> G. Tabbi, W. L. Driessen, J. Reedijk, R. P. Bonomo, N. Veldman, A. L. Spek, *Inorg. Chem.* **1997**, *36*, 1168.  
<sup>[5]</sup> C. J. Campbell, W. L. Driessen, J. Reedijk, W. J. J. Smeets, A. L. Spek, *J. Chem. Soc., Dalton Trans.* **1998**, 2703.  
<sup>[6]</sup> M. Beretta, E. Bouwman, L. Casella, B. Douzdech, W. L. Driessen, L. Gutierrez-Soto, E. Monzani, J. Reedijk, *Inorg. Chim. Acta* **2000**, *310*, 41.

- <sup>[7]</sup> S. J. Lippard, J. M. Berg, *Principles of Bioinorganic Chemistry*, University Science Books, Mill Valley, **1994**.  
<sup>[8]</sup> N. Kitajima, Y. Morooka, *Chem. Rev.* **1994**, *94*, 737.  
<sup>[9]</sup> A. S. Hay, H. S. Stafford, G. F. Endres, J. W. Eustance, *J. Am. Chem. Soc.* **1959**, *81*, 6335.  
<sup>[10]</sup> J. Heijboer, *J. Polym. Sci. C* **1968**, *16*, 3755.  
<sup>[11]</sup> F. E. Karasz, J. M. O'Reilly, *J. Polym. Sci., Pol. Lett.* **1965**, *3*, 561.  
<sup>[12]</sup> P. Gamez, C. Simons, R. Steensma, W. L. Driessen, G. Challa, J. Reedijk, *Eur. Polym. J.* **2001**, *37*, 1293.  
<sup>[13]</sup> A. S. Hay, *J. Polym. Sci.* **1962**, *58*, 581.  
<sup>[14]</sup> H. L. Finkbeiner, A. S. Hay, D. M. White, in: *Polymerization Processes*, vol. XXIV (Ed.: C. E. Schildnecht), Wiley, New York, **1977**, p. 537.  
<sup>[15]</sup> P. J. Baesjou, W. L. Driessen, G. Challa, J. Reedijk, *J. Mol. Catal. A* **1998**, *135*, 273.  
<sup>[16]</sup> P. J. Baesjou, W. L. Driessen, G. Challa, J. Reedijk, *J. Mol. Catal. A* **1999**, *140*, 241.  
<sup>[17]</sup> F. J. Viersen, G. Challa, J. Reedijk, *Polymer* **1990**, *31*, 1368.  
<sup>[18]</sup> P. Gamez, C. Simons, G. Aromí, W. L. Driessen, G. Challa, J. Reedijk, *Appl. Catal. A* **2001**, *214*, 187.  
<sup>[19]</sup> F. J. Viersen, G. Challa, J. Reedijk, *Polymer* **1990**, *31*, 1361.  
<sup>[20]</sup> W. Chen, G. Challa, *Eur. Polym. J.* **1990**, *26*, 1211.

- [21] E. Tsuchida, M. Kaneko, H. Nishide, *Makromol. Chem.* **1972**, 151, 221.
- [22] C. E. Koning, G. Challa, F. B. Hulsbergen, J. Reedijk, *J. Mol. Catal.* **1986**, 34, 355.
- [23] K.-T. Li, *Polym. Bull.* **1995**, 34, 419.
- [24] A. Camus, M. S. Garozzo, N. Marsich, M. Mari, *J. Mol. Catal. A* **1996**, 112, 353.
- [25] P. J. Baesjou, W. L. Driessen, G. Challa, J. Reedijk, *J. Am. Chem. Soc.* **1997**, 119, 12590.
- [26] P. J. Baesjou, PhD Thesis thesis, Leiden University, Leiden, **1997**.
- [27] M. D. Cliff, S. G. Pyne, *Synthesis* **1994**, 681.
- [28] T. Otieno, S. J. Rettig, R. C. Thompson, J. Trotter, *Inorg. Chem.* **1995**, 34, 1718.
- [29] A. W. Addison, T. N. Rao, J. Reedijk, J. van Rijn, G. C. Verschoor, *J. Chem. Soc., Dalton Trans.* **1984**, 1349.
- [30] M. Handa, T. Idehara, K. Nakano, K. Kasuga, M. Mikuriya, N. Matsumoto, M. Kodera, S. Kida, *Bull. Chem. Soc. Jpn.* **1992**, 65, 3241.
- [31] A. R. Oki, J. Sanchez, R. J. Morgan, *J. Coord. Chem.* **1995**, 36, 167.
- [32] K. Nakamoto, in: *Infrared and Raman Spectra of Inorganic and Coordination Compounds*, 4th ed., John Wiley, New York, **1986**, pp. 254.
- [33] B. J. Hathaway, *J. Chem. Soc., Dalton Trans.* **1972**, 1196.
- [34] G. Murphy, P. Nagle, B. Murphy, B. Hathaway, *J. Chem. Soc., Dalton Trans.* **1997**, 2645.
- [35] P. J. Baesjou, W. L. Driessen, G. Challa, J. Reedijk, *J. Mol. Catal. A* **1996**, 110, 195.
- [36] G. M. Sheldrick, *SHELX86, Program for crystal structure determination*, University of Göttingen, Germany, **1986**.
- [37] G. M. Sheldrick, *SHELXL-97-2, Program for crystal structure refinement*, University of Göttingen, Germany, **1996**.
- [38] A. L. Spek, *PLATON, A multi-purpose crystallographic tool*, Utrecht University, The Netherlands, **2002**; internet: <http://www.cryst.chem.uu.nl/platon>
- [39] A. J. C. Wilson (Ed.), *International Tables for Crystallography*, Kluwer Academic Publishers, Dordrecht, The Netherlands, **1992**, vol. C.

Received November 6, 2002  
[I02610]